World Academy of Science, Engineering and Technology
International Journal of Civil and Environmental Engineering
Vol:11, No:2, 2017

Simulation of the Visco-Elasto-Plastic Deformation Behaviour of Short Glass Fibre Reinforced Polyphthalamides

V. Keim, J. Spachtholz, J. Hammer

***Abstract*—**The importance of fibre reinforced plastics continually increases due to the excellent mechanical properties, low material and manufacturing costs combined with significant weight reduction. Today, components are usually designed and calculated numerically by using finite element methods (FEM) to avoid expensive laboratory tests. These programs are based on material models including material specific deformation characteristics. In this research project, material models for short glass fibre reinforced plastics are presented to simulate the visco-elasto-plastic deformation behaviour. Prior to modelling specimens of the material EMS Grivory HTV-5H1, consisting of a Polyphthalamide matrix reinforced by 50wt.-% of short glass fibres, are characterized experimentally in terms of the highly time dependent deformation behaviour of the matrix material. To minimize the experimental effort, the cyclic deformation behaviour under tensile and compressive loading $(R = -1)$ is characterized by isothermal complex low cycle fatigue (CLCF) tests. Combining cycles under two strain amplitudes and strain rates within three orders of magnitude and relaxation intervals into one experiment the visco-elastic deformation is characterized. To identify visco-plastic deformation monotonous tensile tests either displacement controlled or strain controlled (CERT) are compared. All relevant modelling parameters for this complex superposition of simultaneously varying mechanical loadings are quantified by these experiments. Subsequently, two different material models are compared with respect to their accuracy describing the visco-elasto-plastic deformation behaviour. First, based on Chaboche an extended 12 parameter model (EVP-KV2) is used to model cyclic visco-elasto-plasticity at two time scales. The parameters of the model including a total separation of elastic and plastic deformation are obtained by computational optimization using an evolutionary algorithm based on a fitness function called genetic algorithm. Second, the 12 parameter visco-elasto-plastic material model by Launay is used. In detail, the model contains a different type of a flow function based on the definition of the visco-plastic deformation as a part of the overall deformation. The accuracy of the models is verified by corresponding experimental LCF testing.

***Keywords*—**Complex low cycle fatigue, material modelling, short glass fibre reinforced polyphthalamides, visco-elasto-plastic deformation.

I. Introduction

COMPONENTS made of short fibre reinforced plastics are normally produced in their final contour with a high functional integrity by injection moulding. Besides lower costs at higher production rates especially the weight reduction enabled by good mechanical properties at lower density increases the influence of short fibre reinforced plastics for industrial applications.

As a combination of various materials in one structure, the mechanical, chemical and thermal properties of composites are determined by the characteristics of their components. The insufficient mechanical properties of the polymeric matrix are improved by glass fibres. Polyamide provides high stiffness, fatigue strength and resistance to chemicals, influenced by the number of carbon groups between the amide linkages. Synthetic polyamides can be grouped according to the composition of the molecular chains in aliphatic polyamides, aromatic polyamides and polyphthalamides [1]. Polyphthalamides are semi-aromatic polyamides based on the polymerization of terephthalic and isophthalic acid as well as amide. As a matrix material, higher tensile and compressive strength in a temperature range up to $120°\mathrm{C}$ are achieved compared to Polyamide 66. Besides, they provide a high grade shape stability due to less moisture and water absorption [2]. For EMS Grivory HTV-5H1, the Polyphthalamide matrix material is reinforced by 50wt.-% of short, circular glass fibres with a mean diameter of 10 - $15\mu m$.

The overall macroscopic deformation behaviour of the short glass fibre reinforced polyphthalamide is a superposition of the individual deformation mechanisms of the highly non-linear thermoplastic matrix material and the linear-elastic glass fibres. Generally, the modelling of the deformation behaviour of the glass fibres is thereby possible without any difficulties due to their total linear-elastic characteristics. Rather, the interaction between the glass fibres and the matrix material and its high grade temperature- and time-dependent deformation behaviour is the challenging part [3]. For small strains, the material deforms elasticly involving dissipative phenomena affected by relative movements of the molecular chain segments without destroying the chemical bonds normally described by viscosity. This visco-elastic deformation is based on the number of free molecular chains for the movement activated by time depended loadings. For deformation above a specific value irreversible rearrangements of chain segments in semi-crystalline regions occur. Contrary, in the amorphous areas the permanent deformation is a result of bond rotation [4].

The visco-elasto-plastic deformation behaviour is attempted by a huge amount of laboratory tests describing complex mechanical loadings during the service life of the components. As these experiments are expensive and should be aligned difficult to real loads actually, the main issue is to minimize

V. Keim and J. Spachtholz are with the Department of Material Science, Faculty of Mechanical Engineering, OTH Regensburg, 93053 Regensburg, Germany.

J. Hammer is with the Department of Material Science, Faculty of Mechanical Engineering, OTH Regensburg, 93053 Regensburg, Germany (e-mail: joachim.hammer@oth-regensburg.de).

laboratory tests by computational fatigue life time prediction. The fatigue life estimation is usually separated into two parts. First, a material model is essential to simulate the deformation of the material describing all specific effects. Second, a fatigue criterion relying on microscopic damage mechanisms has to be defined.

In the present work, two material models and their parameters identified from one complex experiment for the simulation of the cyclic deformation behaviour of short glass fibre reinforced Polyphthalamide are compared.

II. Experimental Methods

The analysed material is Grivory HTV-5H1 produced by EMS-Grivory (Domat, Swiss). It is a semi-crystalline Polyphthalamide reinforced by 50wt.-% of short glass fibres and black coloured by carbon. Injection moulded specimens according to ISO 527-4 type 1B are used for all tests. The dimensions are given in Fig. 1. In the flat specimens used in the present work, the fibre orientation is held almost parallel to the mould flow direction. The fibre distribution was measured by micro-computer-tomography (GE phoenix v/tome/x s). To ensure constant humidity, the specimens are stored in a climate camper with a relative humidity of 50% and a constant temperature of $25°\mathrm{C}$.

All tests are carried out on a servo hydraulic test rig (MTS 810). The load is measured by a $100kN$ load cell. For the strain controlled tests a contact extensometer (MTS 632.53 F-14) is used. Specimen buckling was observed for compressive loadings. Thus, buckling restraints are used according to the functional requirements mentioned in ISO 12106 which enable cyclic tests under compressive strain amplitudes up $\varepsilon = -1.0 \cdot 10^{-2}$.

The overall cyclic deformation behaviour of fibre reinforced polymers is affected by individual time dependent mechanisms like visco-elasticity and visco-plasticity in various time scales as well as hardening or softening effects [5], [6]. An overview is given by Mortazavian and Fatemi [7]. For the experimental characterization of the deformation effects different tests under various loading conditions are carried out. Following a convenient approach monotonous tensile, cyclic tension-compression and stress relaxation tests are essentially needed. To combine the magnitude of those separate experiments and with the ulterior motive to detect all parameters for the modelling in one complex experiment a modified low cycle fatigue test was published in [8]-[11] as complex low cycle fatigue test (CLCF). The isothermal, strain controlled test includes LCF cycles under different strain rates and strain amplitudes to quantify the overall cyclic visco-elastic deformation behaviour as well as holding times under tensile and compressive loadings for the characterization of relaxation effects. Using the fact that there is no standard for CLCF tests, the original testing procedure for steel and aluminium was modified in order to measure the material response of fibre reinforced plastics. The strain signal of the CLCF test is given in Fig. 2. For the first seven cycles, the strain amplitude is held constant at $\Delta\varepsilon_1/2 = 2.0 \cdot 10^{-3}$. Meanwhile, the strain rate is reduced after five cycles from

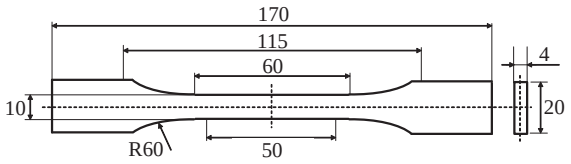

Fig. 1 Injection moulded specimens according to ISO 527-4 type 1B, dimensions in mm

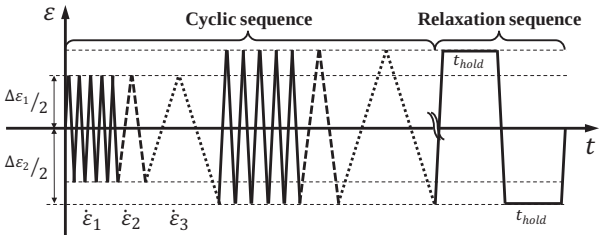

Fig. 2 Strain signal of the modified CLCF test

$\dot{\varepsilon}_1 = 1.31 \cdot 10^{-3} s^{-1}$ by one order of magnitude to $\dot{\varepsilon}_2 = 1.31 \cdot 10^{-4} s^{-1}$. For cycle number seven, the strain rate is further reduced to $\dot{\varepsilon}_3 = 1.31 \cdot 10^{-5} s^{-1}$. Subsequently, the strain amplitude is doubled to $\Delta\varepsilon_2/2 = 4.0 \cdot 10^{-3}$ and the same cycles as defined before are performed. Additional to the cyclic part of the CLCF procedure, two holding times of $t_{hold} = 900s$ are carried out under tensile and compressive loading. This complex superposition of various loading conditions enables the identification of all relevant parameters for the material modelling in one experiment with an overall testing time of $t_{CLCF} = 65min$. To avoid irreversible deformations which influence the visco-elasticity during the CLCF test, the visco-plasticity is experimentally characterized by corresponding tensile tests.

For the characterization of the highly time-dependent plastic deformation, a constant strain rate is required. E.g. Brunbauer et al. [12] and Mortazavian et al. [13] measure the static material properties by displacement controlled tests and assume an equivalent strain rate. The simplification of using a displacement rate instead of a strain rate in their experimental methods is quantified in the present work. The rates are defined corresponding to the CLCF tests.

III. Material Modelling

Modelling the cyclic deformation behaviour of short glass fibre reinforced polymers can basically be realized by two different methods including the microstructure of the material. The scale-transition method is characterized by the separate description of the composite materials. They are linked by microstructural effects to a complete material model [14]. Contrary, the phenomenological approach originally developed for the description of semi-crystalline polymers enables a macroscopic modelling of structural problems physically relied on the deformation behaviour. Combining the visco-elastic material response in the amorphous regions and the visco-plastic deformation in crystalline regions of the polymer, the material behaviour is modelled [15]. The phenomenological models for semi-crystalline polymers are used for fibre reinforced plastics, if the deformation

mechanisms mentioned above exist. The mechanical properties can be regarded as anisotropic for random oriented fibres. For distinct fibre orientations, a relationship between the microstructure and the overall mechanical behaviour is necessary [3], [6], [16]-[18].

A. Visco-Elasto-Plastic Material Model (EVP-KV2) Based on Chaboche

In the literature, several authors simulate the elasto-visco-plastic deformation behaviour of steel and aluminium at higher temperatures sufficiently accurate with the eight parameter Chaboche model (EVP) [4], [8], [19]-[22]. To fit fibre reinforced thermoplastics, Launay et al. [6] added two first order Kelvin-Voigt elements enabling the description of visco-elasticity at two time scales (EVP-KV2).

In the material model, Hooke's Law in rate formulation considers the elastic properties of the material.

$$\dot{\sigma} = E \cdot \dot{\varepsilon}_{el} = E \cdot \left[\dot{\varepsilon} - \sum_{i=1}^{2} \dot{\varepsilon}_{vi} - \dot{\varepsilon}_{vp} \right] \tag{1}$$

The visco-elastic strain rates $\dot{\varepsilon}_{vi}$ at two different time scales are calculated according to:

$$\dot{\varepsilon}_{vi} = \frac{1}{\eta_i} \cdot (\sigma - E_{vi} \cdot \dot{\varepsilon}_{vi}) \qquad i = 1, 2 \tag{2}$$

The characteristic time τ_i of the visco-elasticity thereby is defined as:

$$\tau_i = \frac{\eta_i}{E_{vi}} \qquad i = 1, 2 \tag{3}$$

The decision, whether elastic or plastic deformation is acting, is solved in terms of the flow function f based on the theories of a threshold stress. For $f < 0$ the deformation is held elastic. Plastic material behaviour is defined for $f = 0$.

$$f = |\sigma - \alpha| - R_e - r \tag{4}$$

The product of the equivalent plastic strain rate $\dot{p}$ and the plastic flow direction leads to the visco-plastic strain rate $\dot{\varepsilon}_{vp}$ in case that $f = 0$.

$$\dot{\varepsilon}_{vp} = \dot{p} \cdot \frac{df}{dt} = \dot{\sigma} \cdot sign(\sigma - \alpha) \tag{5}$$

Isotropic hardening effects are considered by a first order linear differential equation. The equivalent plastic strain $\dot{p}$ rate influences the isotropic hardening variable r exponentially.

$$\dot{r} = b \cdot (Q_\infty - r) \cdot \dot{p} \tag{6}$$

Kinematic hardening is considered by a linear first order differential equation according to the constitutive equations by Armstrong and Frederick.

$$\dot{\alpha} = C_\infty \cdot \dot{\varepsilon}_{vp} - \gamma \cdot \dot{p} \cdot \alpha \tag{7}$$

The equivalent plastic strain rate $\dot{p}$ mentioned before is mathematically described by the following relationship called Chaboche's power law:

$$\dot{p} = \left\langle \frac{|\sigma - \alpha| - R_e - r}{K} \right\rangle^{n_0} \tag{8}$$

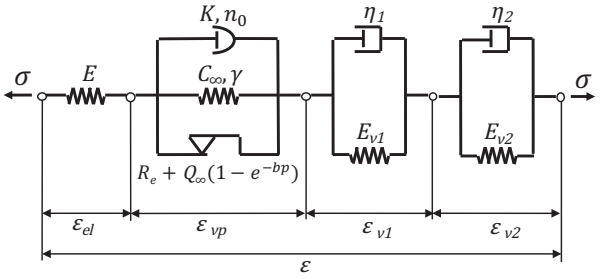

Fig. 3 Rheological scheme of the EVP-KV2 model [6], [22]

The McCauley operators thereby are defined as:

$$\begin{aligned} f(x) < 0 &\longrightarrow \langle f(x) \rangle = 0 \\ f(x) \geq 0 &\longrightarrow \langle f(x) \rangle = f(x) \end{aligned} \tag{9}$$

In the EVP-KV2 model the stress σ, the visco-elastic strain ε_{vi}, the back stress α and the equivalent plastic strain p are state variables. For the description of the deformation mechanisms following parameters are used [6], [22]:

- Linear Elasticity: Young's modulus E,
- Elastic threshold: Yield strength R_e,
- Long-term visco-elasticity: Stiffness modulus E_{v2}, viscosity η_2, characteristic time τ_2,
- Short-term visco-elasticity: Stiffness modulus E_{v1}, viscosity η_1, characteristic time τ_1,
- Isotropic hardening: Hardening modulus Q_∞, exp. b,
- Kinematic hardening: Hardening modulus C_∞, exp. γ,
- Visco-plasticity: Viscosity K exp. n_0,

The analogical scheme of the EVP-KV2 model is given in Fig. 3. Linear-elastic material behaviour is represented by a linear spring element. The visco-plastic deformation behaviour is taken into account by a serially linked parallel connection of a non-linear damper element (viscosity), a spring element (hardening) and a skidding block (threshold stress). Further, visco-elasticity is represented by a serial connection of two first order Kelvin-Voigt elements.

B. Visco-Elasto-Plastic based on Launay

The second material model used to simulate the cyclic deformation behaviour of our material is published by Launay et al. in [6]. Their formulation is based on the generalized standard material (GSM) framework with five variables describing the current mechanical sate (overall stress σ, long-term visco-elastic strain ε_{v1}, short-term visco-elastic strain ε_{v2}, pseudo-visco-plastic strain ε_{vp}, hardening variable $\tilde{\alpha}$, softening variable β). Related to Noda et al. [23] they pronounce changes in the initial stiffness E_e^0 under cyclic loading mathematically described by :

$$E_e(\beta) = g(\beta) \cdot E_e^0 = \left[1 - a \cdot \left(1 - e^{-\beta/\tilde{b}} \right) \right] \cdot E_e^0 \tag{10}$$

Contrary to the EVP-KV2 model, no separation of elastic or plastic deformation by the Yield Strength R_e due to the definition of a pseudo-visco-plastic ε_{vp} deformation as a part of the overall deformation is assumed. Thus, no plastic threshold stress is defined in the material model by

Launay. This is the major difference to the EVP-KV2 model. Further, the flow function is mathematically described by a hyperbolic sine to the power of m, which causes a negligible pseudo-visco-plastic strain rate $\dot{\varepsilon}_{vp}$ for small stresses [16], [24]. Similar to the EVP-KV2 model, the overall stress rate $\dot{\sigma}$ is calculated by Hooke's Law in rate formulation:

$$\dot{\sigma} = E_e(\beta) \cdot \dot{\varepsilon}_{el} = E_e(\beta) \cdot \left[\dot{\varepsilon} - \sum_{i=1}^{2} \dot{\varepsilon}_{vi} - \dot{\varepsilon}_{vp}\right] \tag{11}$$

Visco-elasticity at two time scales is taken into account by two Kelvin-Voigt elements:

$$\dot{\varepsilon}_{vi} = \frac{1}{\eta_i} \cdot (\sigma - E_{vi} \cdot \dot{\varepsilon}_{vi}) \tag{12}$$

$$\tau_i = \frac{\eta_i}{E_{vi}} \qquad i = 1, 2 \tag{13}$$

The pseudo-visco-plastic strain rate $\dot{\varepsilon}_{vp}$ and the rate of the hardening variable $\dot{\tilde{\alpha}}$ are mathematically described by the following differential equations including the hyperbolic sine flow function.

$$\dot{\varepsilon}_{vp} = \tilde{A} \cdot \left[sinh\left(\frac{|\sigma + C \cdot \tilde{\alpha}|}{\tilde{H}}\right)\right]^m \cdot sign\left(\sigma + C \cdot \tilde{\alpha}\right) \tag{14}$$

$$\begin{aligned}\dot{\tilde{\alpha}} = -\tilde{A} \cdot \left[sinh\left(\frac{|\sigma + C \cdot \tilde{\alpha}|}{\tilde{H}}\right)\right]^m \cdot ... \\ ... \cdot \left[sign\left(\sigma + C \cdot \tilde{\alpha}\right) + \tilde{\gamma} \cdot \tilde{\alpha}\right]\end{aligned} \tag{15}$$

The softening variable β physically includes the dissipation of a cumulative energy by the pseudo-visco-plastic effects. In the model it is represented by the following differential equation:

$$\dot{\beta} = \sigma \cdot \dot{\varepsilon}_{vp} - C \cdot \dot{\tilde{\alpha}} \cdot \tilde{\alpha} \tag{16}$$

In the material model following parameters are used for different types of deformation characteristics [6]:

- Linear Elasticity: Initial Young's modulus E_e^0,
- Short-term visco-elasticity: Stiffness modulus E_{v1}, viscosity η_1, characteristic time τ_1,
- Long-term visco-elasticity: Stiffness modulus E_{v2}, viscosity η_2, characteristic time τ_2,
- Hardening effects: Modulus C, parameter $\tilde{\gamma}$,
- Material viscosity: characteristic rate $\tilde{A}$, characteristic stress $\tilde{H}$, exp. m,
- Cyclic softening: Maximal softening a, characteristic energy density b.

In Fig. 4 the material model by Launay et al. [6] can be seen as a rheological network of mechanical elements. The linear-elastic deformation behaviour is represented by a spring element. Visco-plasticity is described by a serially linked parallel connection of a non-linear damper and a non-linear spring element. Similar to the EVP-KV2 model, visco-elastic deformation effects are figured out by two Kelvin-Voigt elements linked in series.

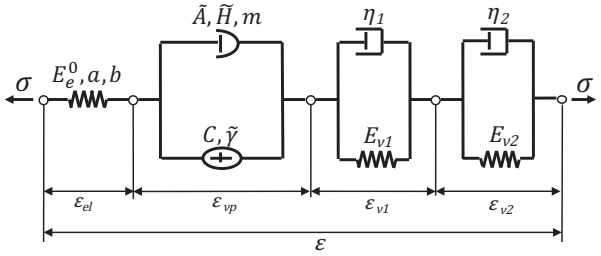

Fig. 4 Rheological scheme of the material model by Launay et al. [6]

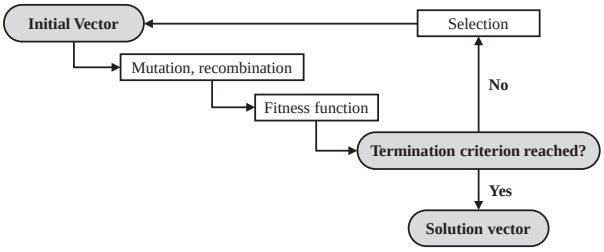

Fig. 5 Basic structure of the optimization tool used in the present work

C. Parameter's Optimization

The parameters of the two material models are optimized by the approximation of the calculated stress curves and the measured stress curves. In a first step, all parameters of the material models are fitted to the isothermal CLCF test. Subsequently, the visco-elastic parameters are held constant while optimizing the visco-plastic parameters to the CERT. This proceeding is reasoned by possible material fatigue for higher loadings defined for the CLCF test.

The equations of the material models are integrated by the Euler-Forward-Method and brought into the optimization tool. Due to long computation times and their sensitivity on the initial set of parameters by Levenberg-Marquard methods, an evolutionary algorithm based on a fitness function (genetic algorithm) is used. These algorithms are attributed on the biodiversity attributed to the biological evolution (Darwin's theories) [25]-[27]. At the beginning of the optimization a random initial set of parameters called parent vector is defined within physically reliable boundaries. The descendant vectors are formed by mutation and recombination of the parent vector. The population is the combination of the initial vector and its descendants, which stands for one iteration step of the optimization problem. Selected by their quality the best fitting descendants (elite) are used as initial vectors for the next iteration step. Other vectors are not considered further and replaced by mutation and recombination of the parent vector. A fitness function based on least squares is implemented [28]-[31]. The basic structure of the optimization tool is given in Fig. 5.

IV. Results

A. Comparison of Displacement and Strain Controlled Tensile Tests

In Fig. 8, the displacement and strain controlled tensile tests are compared for a displacement rate $v = 1mm/min$ and a strain rate $\dot{\varepsilon}_2 = 1.31 \cdot 10^{-4} s^{-1}$. The difference in the measured

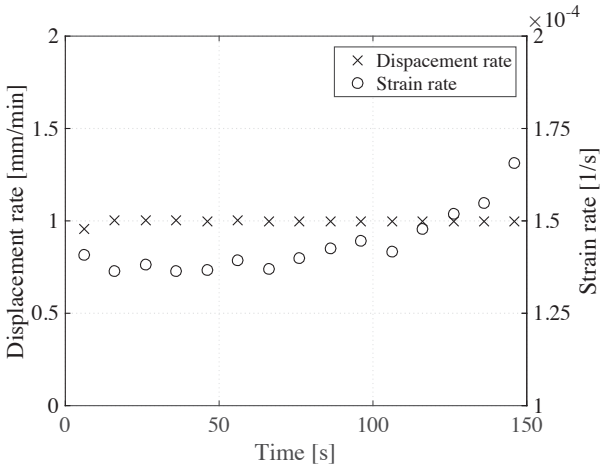

Fig. 6 Displacement rate (control signal) and measured strain rate during a tensile test ($v = 1mm/min$)

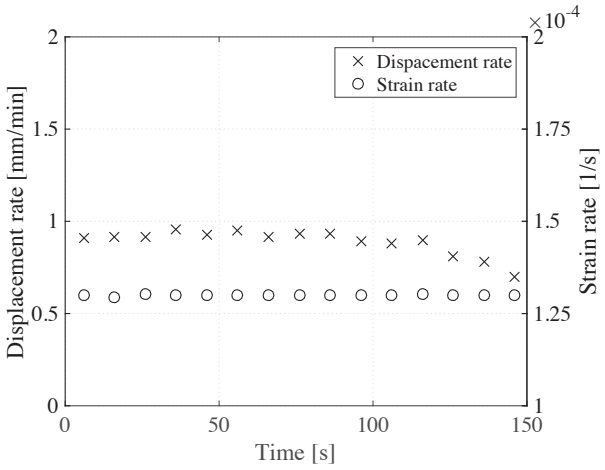

Fig. 7 Strain rate (control signal) and measured displacement rate during a CERT ($\dot{\varepsilon}_2 = 1.31 \cdot 10^{-4} s^{-1}$)

stress strain curves is explained by the time dependent plastic deformation behaviour of the material. A significant reduction of the tensile strength from $R_m = 260MPa$ (displacement controlled) to $R_m = 250MPa$ (CERT) is observed. Further, a slight deviation in the fracture strain is visible.

As shown in Fig. 6 for a constant displacement rate, the measured strain rate increases while plastic deformation occurs. Contrary in Fig. 7 for a constant strain rate, the measured displacement rate decreases by at least one third. There is less stress relaxation caused by enhanced strain rate in displacement controlled tensile tests. Therefore, the tensile strength is about $10MPa$ higher. These effects are observed for strain rate controlled tensile tests (CERT) vice versa. For elastic deformation no changes distinguished in the diagrams are noted.

B. Identification of the Parameters for the Material Model EVP-KV2

In Fig. 9, the complete experimental measured stress response is compared to the results of the optimization with the EVP-KV2 model for the CLCF strain control signal according

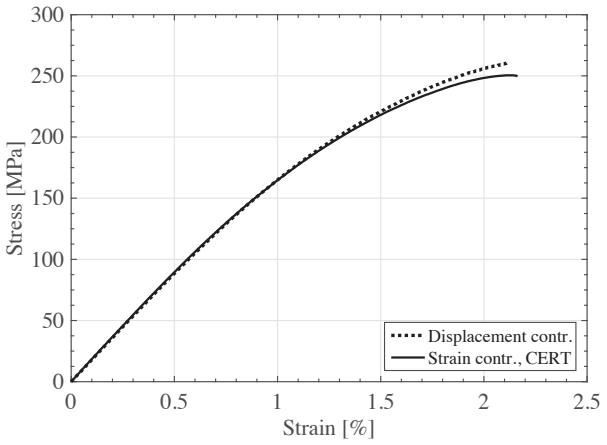

Fig. 8 Comparison of the stress-strain-curves measured by a displacement controlled tensile test ($v = 1mm/min$) and a strain controlled CERT ($\dot{\varepsilon}_2 = 1.31 \cdot 10^{-4} s^{-1}$)

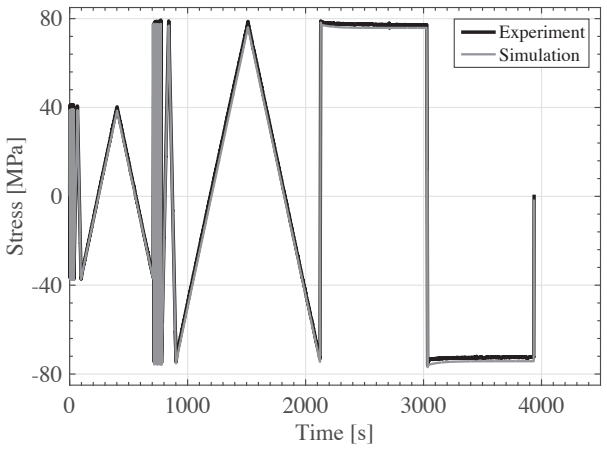

Fig. 9 Simulation of the complete CLCF test by the material model EVP-KV2

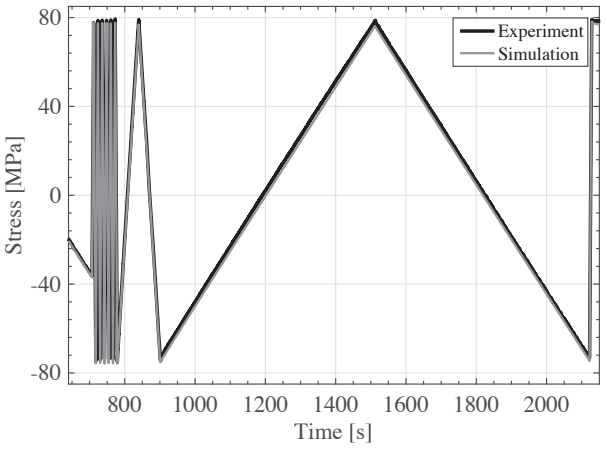

Fig. 10 Simulation of the CLCF test by the EVP-KV2 model, cyclic part at $\Delta\varepsilon_2/2 = 4.0 \cdot 10^{-3}$

to Fig. 2. The model describes the visco-elastic cyclic loading under two strain amplitudes and strain rates within three orders of magnitude as well as the stress relaxation under tensile and compressive load sufficiently accurate. By using a genetic algorithm, the calculation time for the parameter identification

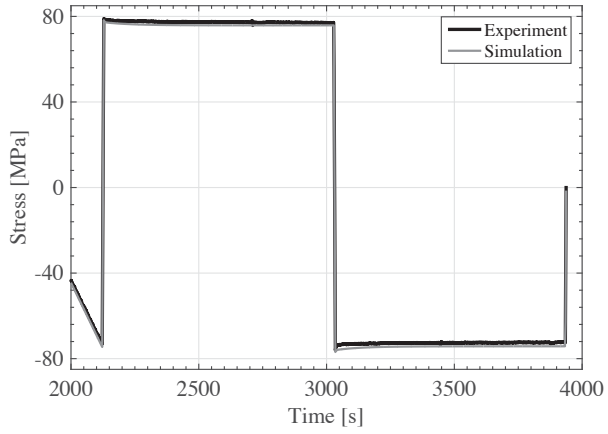

Fig. 11 Simulation of the relaxation sequence by the EVP-KV2 model

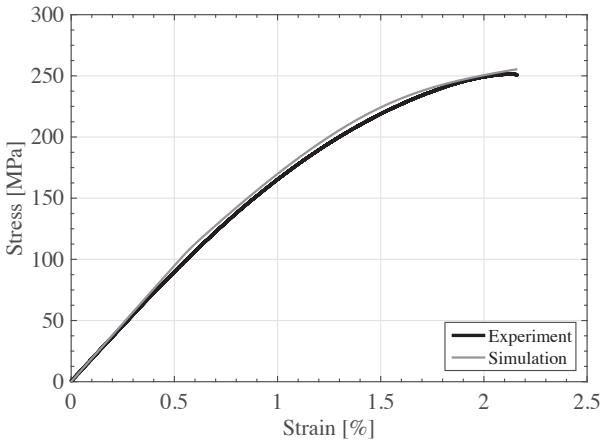

Fig. 12 Simulation of the CERT by the EVP-KV2 model

is about $3'000s$ with total sum of least squares is $388'290$.

Fig. 10 shows seven cycles at a constant strain amplitude of $\Delta\varepsilon_2/2 = 4.0 \cdot 10^{-3}$ and three strain rates. For strain rates $\dot{\varepsilon}_1 = 1.31 \cdot 10^{-3}s^{-1}$ and $\dot{\varepsilon}_2 = 1.31 \cdot 10^{-4}s^{-1}$ the maximum difference between the simulated and the measured stress curves is about $1.1MPa$ (deviation: 1.4%) at the load reversal points. At a strain rate of $\dot{\varepsilon}_3 = 1.31 \cdot 10^{-5}s^{-1}$ the EVP-KV2 model underestimates the measured stress values by $2.7MPa$ (deviation: 3.4%), which represents the maximum difference between the experiment and the simulation.

In Fig. 11, the complete relaxation part in tension and compression is shown. The transition into the hold time sequences and the relaxation behaviour is in satisfying congruence. The maximum difference is about $1.9MPa$ (deviation: 2.5%). The EVP-KV2 model simulates the changes in the relaxation rates exactly by the visco-elastic parameters at two time scales (Kelvin-Voigt elements).

The measured and calculated stress strain curve (Fig. 12) from the CERT test with a strain rate of $\dot{\varepsilon}_2 = 1.31 \cdot 10^{-4}s^{-1}$ shows the accurate description of the visco-elasto-plastic deformation behaviour. The maximum difference is $4MPa$ (deviation: 1.8%). The EVP-KV2 model simulates the complete deformation including the tensile strength. The sum of least squares for the simulation of the CERT is computed to $281'400$. The identified set of parameters for the EVP-KV2 model describing Grivory HTV-5H1 is given in Table I.

TABLE I
IDENTIFIED PARAMETERS OF THE EVP-KV2 MODEL

Parameter	Symbol	Unit	
Initial Young's modulus	E	MPa	$1.92 \cdot 10^4$
Yield Stress	R_e	MPa	86.6
Short-term visco-elasticity			
Stiffness modulus	E_{v1}	MPa	$1.41 \cdot 10^6$
Viscosity	η_1	$MPas$	$4.60 \cdot 10^6$
Characteristic time	τ_1	s	3.2
Long-term visco-elasticity			
Stiffness modulus	E_{v2}	MPa	$1.57 \cdot 10^6$
Viscosity	η_2	$MPas$	$1.66 \cdot 10^8$
Characteristic time	τ_2	s	105.8
Isotropic hardening			
	Q_∞	MPa	389.0
	b	$-$	7.5
Kinematic hardening			
	C_∞	MPa	$7.53 \cdot 10^4$
	γ	$-$	636.4
Material viscosity			
Viscosity	K	MPa	120.1
Exponent	n_0	$-$	6.2

C. Identification of the Parameters for the Launay Model

In analogy to the EVP-KV2 model, in Fig. 13, the complete stress response measured by the isothermal CLCF test is compared to the simulation results the Launay model. Again, the visco-elasticity at two times scales as well as the visco-plasticity under cyclic and monotonic loadings are simulated in satisfying congruence. The parameter identification by the genetic algorithm takes about $9'100$s. The computed sum of least squares for the complete simulation of the CLCF test is $513'670$.

In Fig. 14, seven cycles under a constant strain amplitude of $\Delta\varepsilon_2/2 = 4.0 \cdot 10^{-3}$ and three strain rates are shown. The maximum difference at the load reversal points between the simulation and the experiment is $2.1MPa$ (deviation: 2.6%). Similar to the EVP-KV2 model, the Launay model underestimates the experimentally measured stress values for the cycle under $\dot{\varepsilon}_3 = 1.31 \cdot 10^{-5}s^{-1}$ by $2.0MPa$, which is a deviation of about 2.5%.

Fig. 15 shows the simulation of the relaxation sequences under tensile and compressive loadings. The peak stress during the transition into the tensile hold time is underestimated by $1.3MPa$ (deviation: 1.6%). Contrary, the peak stress is overestimated by $1MPa$ (deviation: 1.3%) at the transition into the compressive hold time. During the tensile holding time the maximum difference between the simulation and the test is about $1MPa$ (deviation: 1.3%). This difference is significantly higher for the compressive hold time ($3MPa$, deviation: 4.0%). The relaxation rates at the beginning of the relaxation intervals are slightly overestimated by the Launay model caused by a high-grade short-term visco-elasticity.

The comparison of the simulation experimental results of the CERT test are given in Fig. 16. Similar to the CLCF test,

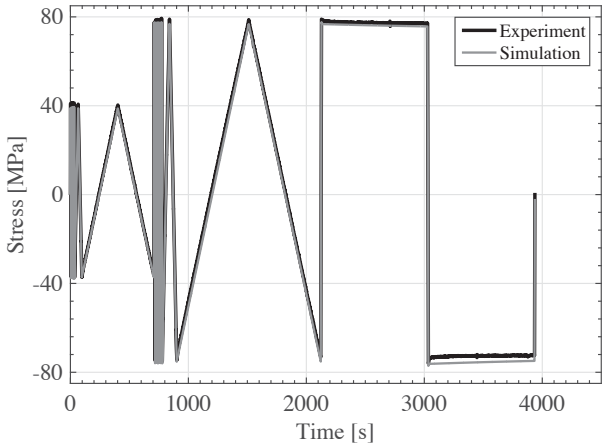

Fig. 13 Simulation of the complete CLCF test by the Launay model

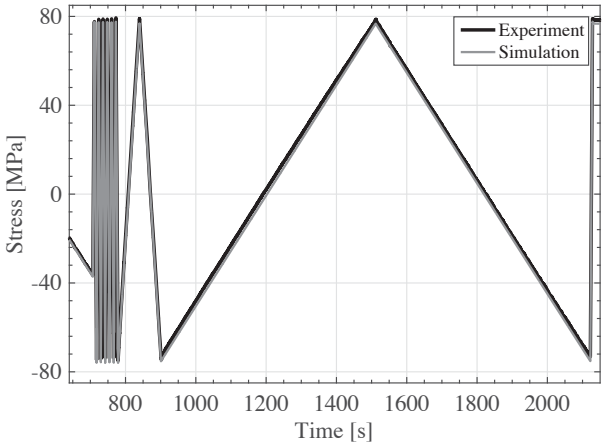

Fig. 14 Simulation of the cyclic part at strain amplitude $\Delta\varepsilon_2/2 = 4.0 \cdot 10^{-3}$ by the Launay model

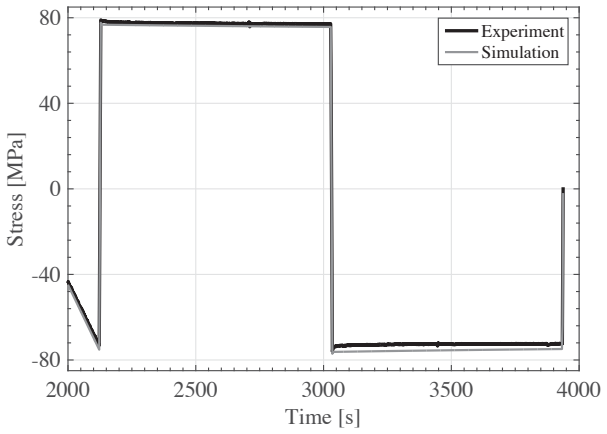

Fig. 15 Simulation of the relaxation sequence by the Launay model

the visco-elastic deformation behaviour is well simulated by the Launay model. Insufficient accuracy is observed for the visco-plastic deformation with a maximum difference between the measured and simulated stress strain curve of $9MPa$ (deviation: 3.9%). Similar to the EVP-KV2 model the tensile strength and the fracture strain are accurately simulated. The sum of least squares for the simulation of the CERT by

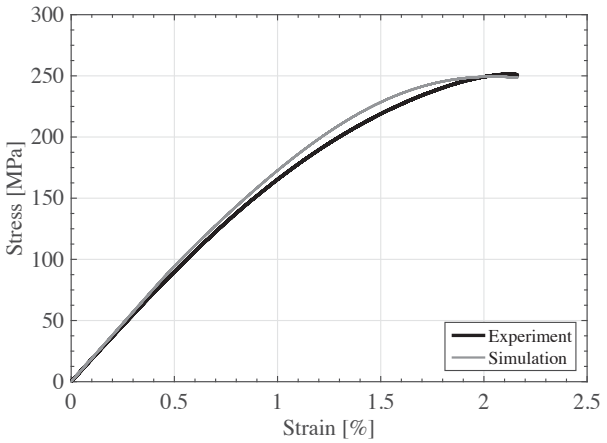

Fig. 16 Simulation of the CERT ($\dot{\varepsilon}_2 = 1.31 \cdot 10^{-4} s^{-1}$) by the Launay model

TABLE II
IDENTIFIED PARAMETERS OF THE LAUNAY MODEL

Parameter	Symbol	Unit	
Initial Young's modulus	E_e^0	MPa	$1.93 \cdot 10^4$
Long-term visco-elasticity			
Stiffness modulus	E_{v1}	MPa	$2.51 \cdot 10^6$
Viscosity	η_1	$MPas$	$3.67 \cdot 10^9$
Characteristic time	τ_1	s	1462.1
Short-term visco-elasticity			
Stiffness modulus	E_{v2}	MPa	$9.89 \cdot 10^5$
Viscosity	η_2	$MPas$	$1.89 \cdot 10^6$
Characteristic time	τ_2	s	1.9
Non-linear hardening			
Hardening modulus	C	MPa	$1.65 \cdot 10^5$
Non-linear parameter	$\tilde{\gamma}$	$-$	978.
Non-linear viscosity			
Characteristic rate	$\tilde{A}$	s^{-1}	$8.19 \cdot 10^{-10}$
Characteristic stress	$\tilde{H}$	MPa	44.9
Exponent	m	$-$	7.32
Cyclic softening			
Maximal softening	a	$\%$	198
Energy density	$\tilde{b}$	Jm^{-3}	102

the Launay model is $626'800$. The identified parameters for the Launay model simulating the deformation behaviour of Grivory HTV-5H1 are shown in Table II.

V. DISCUSSION

The comparison of displacement controlled and strain controlled (CERT) tensile tests leads to the fact, that even for room temperature the plastic deformation behaviour is highly time dependent. The modelling of the time-dependent deformation is essentially based on a constant deformation or rather strain rate. For other control modes the stress response including tensile strength and the fracture strain are the most influenced static material parameters. The simplification of equivalent strain rates [7], [12] significantly decreases the accuracy of the modelling.

Contrary to a convenient approach, using one complex experiment (CLCF) for the identification of the parameters

TABLE III
COMPUTED SUM OF LEAST SQUARES FOR THE PROPOSED MATERIAL MODELS SIMULATING THE CLCF TEST AND CERT

	EVP-KV2	**Launay**
CLCF	388'290	513'670
CERT	281'400	626'800
Σ	**669'690**	**1'140'470**

enables an economical alternative. In the present work, the idea of a modified low cycle fatigue test [8]-[11] is used for to experimentally characterize the deformation behaviour of fibre reinforced plastics for the first time. Basically the identification of all relevant visco-elasto-plastic parameters for the modelling is possible. Due to a defined elastic cyclic load case, only the visco-elastic parameters are identified by the CLCF experiment. Material damage by cyclic plasticity decreases the accuracy of the parameter identification. Thus, the visco-plastic parameters of material models are identified by a CERT under a corresponding strain rate.

The Levenberg-Marquard optimization method mainly used in literature [6], [22] is replaced by a genetic algorithm. Thereby the computation time as well as the sensitivity on the initial set of parameters are minimized. Its fitness function is based on the computation of the sum of least squares.

In Table III, the sum of least squares for the simulations of the CLCF test and CERT by the EVP-KV2 and the Launay model are given. Best results for the simulation at room temperature are obtained for the EVP-KV2 model with a total sum of $669'690$, which is about one half compared to the Launay model.

One of the most significant advantages of the EVP-KV2 model describing the cyclic deformation behaviour of materials is the flow function including the separation of elastic and plastic deformation by the Yield Strength R_e. Thus, no visco-plastic deformation results, when stresses below the optimized parameter Yield Strength $R_e = 86MPa$ are calculated. For $f < 0$ the overall deformation is held elastic or rather visco-elastic. If the current stress state exceeds the Yield Strength R_e, the overall deformation is a combination of elastic, visco-elastic and visco-plastic effects. This is mathematically described by Chaboche's power law (8). Contrary, in the material model form Launay et al. [6] based on a flow function including a hyperbolic sine (Delobelle's theories) the visco-plastic deformation is held as a part of the overall deformation without any specific separation (14).

VI. CONCLUSION

In the present work a comparison of two different material models regarding to their accuracy describing the cyclic deformation behaviour of Grivory HTV-5H1 is successfully realized. For the simulation at room temperature the definition of the visco-plastic strain as a part of the overall strain in the Launay model causes slightly worse results. Although Launay et al. [6] propose better results for their model, in the present work the best simulation results are observed for the EVP-KV2 model including a total separation of elastic and plastic deformation. As a result of the present work, both models enable the description of the time-dependent stress response at room temperature.

ACKNOWLEDGMENT

The authors wish to express their appreciation to all members of the Laboratory of Material Science at OTH Regensburg for their scientific support and their experimental assistance.

REFERENCES

[1] C. A. Harper, *Handbook of Plastic Processes*, 1st ed. John Wiley & Sons, 2006.
[2] T. Jeltsch, "Metal replacement - To the limits of the possible," *Kunststoffe international*, pp. 88–90, Aug. 2007.
[3] Y. Rémond, "Constitutive modelling of viscoelastic unloading of short glass fibre-reinforced polyethylene," *Composites Science and Technology*, vol. 65, no. 3–4, pp. 421–428, 2005.
[4] L. Lemaitre and J. Chaboche, *Mechanics of solid materials*. Chambridge University Press, 1990.
[5] A. Launay, Y. Marco, M. H. Maitournam, I. Raoult, and F. Szmytka, "Cyclic behavior of short glass fiber reinforced polyamide for fatigue life prediction of automotive components," *Procedia Engineering*, vol. 2, no. 1, pp. 901–910, 2010.
[6] A. Launay, M. H. Maitournam, Y. Marco, I. Raoult, and F. Szmytka, "Cyclic behaviour of short glass fibre reinforced polyamide: Experimental study and constitutive equations," *International Journal of Plasticity*, vol. 27, no. 8, pp. 1267–1293, 2011.
[7] S. Mortazavian and A. Fatemi, "Fatigue behavior and modeling of short fiber reinforced polymer composites: A literature review," *International Journal of Fatigue*, vol. 70, pp. 297–321, 2015.
[8] C. Schweizer, "Physikalisch basierte Modelle für Ermüdungsrisswachstum und Anrisslebensdauer unter thermischen und mechanischen Belastungen," Ph.D. dissertation, KIT, Kalsruhe, 2013.
[9] T. Seifert, M. Borsutzki, and S. Geisler, "Ein komplexes LCF-Versuchsprogramm zur schnellen und günstigen Werkstoffparameteridentifizierung," *Fortschritte der Kennwertermittlung in Forschung und Praxis*, 2006.
[10] T. Seifert, C. Schweizer, M. Schlesinger, M. Möser, and M. Eibl, "Thermomechanical fatigue of 1.4849 cast steel – experiments and life prediction using a fracture mechanics approach," *International Journal of Materials Research*, vol. 101, no. 8, pp. 942–950, 2010.
[11] T. Seifert, "Simulation von Hochtemperaturbauteilen mittels FEM," Freiburg, May 2012.
[12] J. Brunbauer, A. Mösenbacher, C. Guster, and G. Pinter, "Fundamental influences on quasistatic and cyclic material behavior of short glass fiber reinforced polyamide illustrated on microscopic scale," *Journal of Applied Polymer Science*, vol. 131, no. 19, Oct. 2014.
[13] S. Mortazavian and A. Fatemi, "Effects of fiber orientation and anisotropy on tensile strength and elastic modulus of short fiber reinforced polymer composites," *Composites Part B: Engineering*, vol. 72, pp. 116–129, 2015.
[14] S. G. Advani and C. L. T. Iii, "The Use of Tensors to Describe and Predict Fiber Orientation in Short Fiber Composites," *Journal of Rheology (1978-present)*, vol. 31, no. 8, pp. 751–784, Nov. 1987.
[15] G. Ayoub, F. Zaïri, M. Naït-Abdelaziz, and J. M. Gloaguen, "Modelling large deformation behaviour under loading–unloading of semicrystalline polymers: Application to a high density polyethylene," *International Journal of Plasticity*, vol. 26, no. 3, pp. 329–347, 2010.
[16] J.-L. Chaboche, "Thermodynamic formulation of constitutive equations and application to the viscoplasticity and viscoelasticity of metals and polymers," *International Journal of Solids and Structures*, vol. 34, no. 18, pp. 2239–2254, 1997.
[17] A. Drozdov, A. Al-Mulla, and R. Gupta, "The viscoelastic and viscoplastic behavior of polymer composites: polycarbonate reinforced with short glass fibers," *Computational Materials Science*, vol. 28, no. 1, pp. 16–30, 2003.
[18] A. D. Drozdov, A. Al-Mulla, and R. K. Gupta, "Finite viscoplasticity of polycarbonate reinforced with short glass fibers," *Mechanics of Materials*, vol. 37, no. 4, pp. 473–491, 2005.
[19] J.-L. Chaboche and F. Gallerneau, "An overview of the damage approach of durability modelling at elevated temperature," *Fatigue & Fracture of*

Engineering Materials & Structures, vol. 24, no. 6, pp. 405–418, Jun. 2001.
[20] F. Dunne and N. Petrinic, *Introduction to computational plasticity*. Oxford: Oxford University Press, 2005.
[21] J. C. Simo and T. J. R. Hughes, *Computational Inelasticity*, 7th ed. Stanford: Springer Berlin, Heidelberg, 2000.
[22] F. Wilhelm, J. Spachtholz, M. Wagner, C. Kliemt, and J. Hammer, "Simulation of the Viscoplastic Material Behaviour of Cast Aluminium Alloys due to Thermal-Mechanical Loading," *Journal of Materials Science and Engineering. A*, vol. 4, no. 1A, 2014.
[23] K. Noda, A. Takahara, and T. Kajiyama, "Fatigue failure mechanisms of short glass-fiber reinforced nylon 66 based on nonlinear dynamic viscoelastic measurement," *Polymer*, vol. 42, no. 13, pp. 5803–5811, 2001.
[24] P. Germain, Q. S. Nguyen, and P. Suquet, "Continuum Thermodynamics," *Journal of Applied Mechanics*, vol. 105, pp. 1010–1021, Dec. 1983.
[25] S. N. Sivanandam and S. N. Deepa, *Introduction in genetic algorithms*. Springer Berlin Heidelberg, 2008.
[26] X. Yu, *Introduction to Evolutionary Algorithms*. Springer London, 2010.
[27] K. Kraßnitzer, *Lösung des Traveling-Salesmans-Problems mittels eines genetischen Algorithmus auf einem HPC-Cluster*, 1st ed. Grin Verlag, 2013.
[28] A. J. Chipperfield, P. J. Fleming, and C. M. Fonseca, "Genetic Algorithm Tools for Control Systems Engineering," *ResearchGate*, vol. 23, no. 3, Jan. 1994.
[29] E. A. Eiben and J. Smith, *Introduction to evolutionary computing*, 1st ed. Springer, 2003.
[30] B. Kost, *Optimierung mit Evolutionsstrategien*, 1st ed. Hamburg: Harri Deutsch, 2003.
[31] P. Natterer, *Philisophie der Biologie*, 1st ed. Books on Demand, 2010.